



**HAL**  
open science

## Observations of a sky Lyman $\alpha$ groove related to enhanced solar wind mass flux in the neutral sheet

Jean-Loup Bertaux, Eric Quémerais, Rosine Lallement

### ► To cite this version:

Jean-Loup Bertaux, Eric Quémerais, Rosine Lallement. Observations of a sky Lyman  $\alpha$  groove related to enhanced solar wind mass flux in the neutral sheet. *Geophysical Research Letters*, 1996, 23 (25), pp.3675-3678. 10.1029/96GL03475 . insu-04748942

**HAL Id: insu-04748942**

**<https://insu.hal.science/insu-04748942v1>**

Submitted on 24 Oct 2024

**HAL** is a multi-disciplinary open access archive for the deposit and dissemination of scientific research documents, whether they are published or not. The documents may come from teaching and research institutions in France or abroad, or from public or private research centers.

L'archive ouverte pluridisciplinaire **HAL**, est destinée au dépôt et à la diffusion de documents scientifiques de niveau recherche, publiés ou non, émanant des établissements d'enseignement et de recherche français ou étrangers, des laboratoires publics ou privés.

Copyright

# Observations of a sky Lyman $\alpha$ groove related to enhanced solar wind mass flux in the neutral sheet

Jean-Loup Bertaux , Eric Quémerais and Rosine Lallement

Service d'Aéronomie du CNRS, BP 3,91371 Verrières-le-Buisson, FRANCE

**Abstract.** We report several observations of the  $L\alpha$  interplanetary emission recorded by a photometer flown in 1977 on board the soviet spacecraft Prognoz-5. The Prognoz scans sampled emission in a plane perpendicular to the sun-spacecraft line and also traversed the  $L\alpha$  maximum emission region (MER), a region centered a few AU from the Sun on the upstream interstellar-flow axis. These scans reveal the existence of a 10% decrease in intensity centered near the ecliptic plane and about  $30^\circ$  wide. All the dips form a new feature of the interplanetary emission, a "groove" aligned approximately with the ecliptic plane. This groove is present only near the upwind direction, and is interpreted as the result of enhanced ionisation of interstellar H by charge-exchange with the solar wind in a sheet of approximately  $30^\circ$  width in latitude around the average position of the neutral sheet , at this time of solar minimum.

## Introduction

Near the Sun, the flow of interstellar neutral H atoms is characterized by a temperature of 8,000 K, and a velocity vector of 20 km/s, coming from the direction  $\text{long}_{\text{ec}} = 252^\circ$ ,  $\text{lat}_{\text{ec}} = +7^\circ$  in ecliptic coordinates (Bertaux *et al.*, 1985), therefore very near the ecliptic plane. These H atoms are destroyed by EUV photo-ionization (accounting for about 20% of the destruction) and by charge-exchange with protons in the solar wind, which is the main destruction effect. The newly created H neutrals with the radial velocity of the solar wind are not illuminated by the solar  $L\alpha$  line because of their Doppler shift and do not participate to the interplanetary  $L\alpha$  emission, while all the other H atoms which have not been destroyed are scattering solar  $L\alpha$  photons at a rate of  $g_0 = 1.8 \cdot 10^{-3} \text{ s}^{-1}$  at 1 A.U.

As a result, a cavity of ionization is carved into the flow of H atoms, elongated in the downwind direction (opposite to their incoming direction). Given the ionization rate by the solar wind, the resulting H density distribution in the solar system can be modelled, and the interplanetary  $L\alpha$  emissivity (number of photons emitted per  $\text{cm}^{-3}$  per second) may then be calculated by multiplying the H density distribution by  $g_0 / r^2$  (in the optically thin approximation). A map of this emissivity distribution is represented in fig.1 under the form of iso-emissivity contours, computed with the assumption of a spherically symmetric ionization (so-called isotropic solar wind). In such a case, both the H density and emissivity have a symmetry of revolution around the wind axis, and can be represented in a plane, overlotted on the ecliptic plane in fig.1. The main feature of this emissivity pattern is a broad

maximum region, called the MER (Maximum Emissivity Region, Lallement *et al.*, 1991), located upstream of the sun, centered on the wind axis at a distance of a few A.U. In this region, atoms can approach nearer the sun because they arrive directly from outside.

Intensity measurements can be compared to calculated maps of  $L\alpha$  emission (by integration of emissivity along the line of sight), plotted under the form of iso-intensity contours, as the example shown in figure 2 in Rayleigh unit ( $1 \text{ R} = 10^6 / 4\pi \text{ photons cm}^{-2} \text{ s}^{-1} \text{ sr}^{-1}$ ). The main feature of this emission distribution is its dipole character, with a broad maximum around the MER and the upwind direction and a minimum in the downwind direction, consistent with the distribution of emissivity of fig.1.

A second feature of the  $L\alpha$  sky emission is an enhancement of the emission near the ecliptic poles, related to the fact that the solar wind ionization rate is smaller at high latitudes than in the ecliptic plane. This feature is best observed from a position located downwind from the sun in the solar system, which was the case for the discovery observations by Mariner 10 (Kumar and Broadfoot, 1979) and Prognoz (Lallement *et al.*, 1985).

The purpose of this paper is to present Prognoz  $L\alpha$  observations which show the existence of a third feature in the pattern of the interplanetary  $L\alpha$ : a small dip of the emission extending over  $30\text{-}40^\circ$  of ecliptic latitude across the region of maximum emission, aligned along the ecliptic

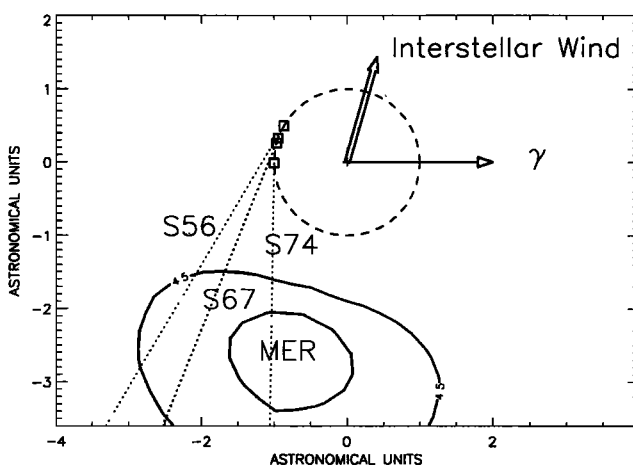


Figure 1. A model distribution of  $L\alpha$  emissivity is shown (in units of number of photons emitted per sec per  $\text{m}^3$ ), overlotted on the ecliptic plane. Only iso-contours defining the MER (Maximum Emissivity Region) are displayed. The positions of Prognoz 5 are indicated, together with the projections of the scan planes where  $L\alpha$  distributions of figure 3 were obtained.

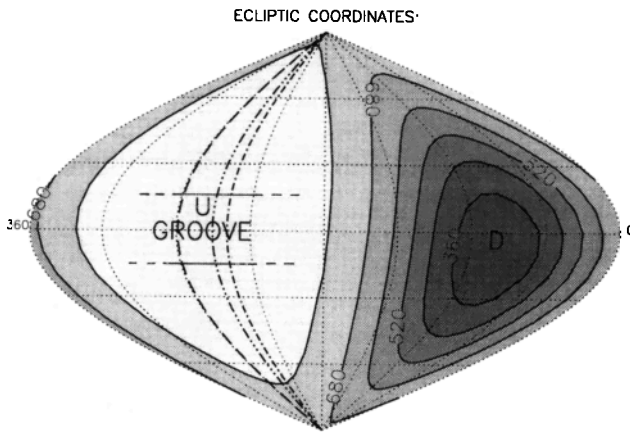


Figure 2. Model distribution of  $L\alpha$  intensity pattern over the sky in ecliptic coordinates. Iso-intensity contours are in Rayleigh; brighter on the plot means brighter in the sky. The model assumed that the observer was at the position of the Sun, with an isotropic ionization rate. Letters U and D indicate respectively the Upwind (from where the wind blows) and Downwind directions. The pattern is characterized by a dipole-type distribution, with the maximum intensity centered around U. The trace of Prognoz scan planes are indicated by dash-dot lines and the position of the observed groove is indicated between two horizontal lines.

plane as a groove ploughed in the emission pattern. This  $L\alpha$  groove is interpreted as the result of enhanced ionization of incoming interstellar H atoms by the solar wind in a thin band of ecliptic latitude, produced by the slow solar wind concentrated in the neutral sheet, flat and thin at the time of the 1976 solar minimum. Such a  $L\alpha$  dip observed by Prognoz was already mentioned in the SWAN proposal to ESA for the SOHO mission (Bertaux *et al.*, 1987, 1989) as a potentially important means of diagnostic for the structure of the solar wind.

#### Lyman alpha observations of the groove with Prognoz-5

The french  $L\alpha$  photometer flown on soviet satellites Prognoz-5 and 6 has been described elsewhere in detail (Bertaux *et al.*, 1985). It is a photomultiplier tube with a 100 Å filter centered at 1216 Å, with an instantaneous field of view of  $2 \times 5^\circ$ , and one second counting time of the photon pulses every 20 second. The optical axis is oriented perpendicular to the spin axis of the spacecraft, which is itself pointed to the sun (within a few degrees), recording the  $L\alpha$  intensity along a great circle perpendicular to the ecliptic plane. The spin rate is 3 °/s. The apogee distance is 200,000 km, and the data presented here were obtained near the apogee of 3 orbits of Prognoz-5, at positions in the Solar system indicated in fig. 1. Each data set consists of the distribution of the measured interplanetary intensity along a great circle whose projection is also indicated on fig.1. They are displayed in fig.3 as a function of the scan angle of the spacecraft, with 0 and  $180^\circ$  corresponding to the ecliptic plane,  $90^\circ$  and  $270^\circ$  corresponding respectively to the North and South ecliptic poles.

The large apogee distance allowed to get the spacecraft out of the geocorona (a strong source of  $L\alpha$  radiation) and to observe the interplanetary  $L\alpha$  emission without any geocoronal emission on a substantial part of the sky. Still, in order to get the interplanetary emission in other parts of the

sky contaminated by geocoronal emission, two methods were used to arrive at data of figure 3. For session S-56 (discussed in terms of solar wind latitude distribution in Lallement *et al.* (1985) under the name S-5), the geocoronal signal was determined by measuring the variation with the distance of the spacecraft to the Earth when looking in a fixed direction, as described in Bertaux *et al.* (1985).

The other  $L\alpha$  distributions presented here show the geocoronal emission subtracted by another method, which makes use of the existence of one Hydrogen absorption cell in the light path of the Prognoz instrument. When the H cell is turned ON, it acts as a negative filter blocking all photons around  $L\alpha$  (121.566 nm) lying within  $2 \cdot 10^{-3}$  nm of line center, in the reference system of the instrument. When the spacecraft is near the apogee, its Doppler shift is negligible with geocoronal atoms, and also the temperature of these atoms is relatively small at large distance; therefore, the H cell absorbs completely the geocoronal emission, except in a few cases when the line of sight approaches the Earth's center (fig 3). Since these cases are located near the direction of the South ecliptic pole, it does not affect the groove which lies near the ecliptic plane.

The H cell does affect the interplanetary emission, but only in limited portions of the sky near the ecliptic poles where the Doppler shift with the wind is small. As can be understood from the configuration of observations of fig.1, at the locations of the Earth for Prognoz-5 data, the combined motions of the Earth (30 km/s) and the interstellar wind (20 km/s) give a substantial doppler shift (with no more H cell absorption), except in the directions perpendicular to the combined motion, near the ecliptic poles, where depressions of 30 % can be seen near scan angles of  $90^\circ$ , and less clearly around  $270^\circ$  due to the interference of the non-absorbed geocoronal signal. In the portion between scan angles  $120^\circ$  and  $240^\circ$ , the doppler shift exceeds the absorption width of the H cell and the recorded signal is the pure interplanetary signal, except for a few points where a hot star, duly identified, gives an extra signal.

The S/N ratio follows the  $n^{0.5}$  statistics. Curves of fig.3 were obtained from six hours of data, corresponding to 180 spacecraft rotations and 1080 individual measurements spread over a great circle. In average, six individual measurements were binned in every  $2^\circ$  bin of scan angle, and the resulting average number of photons counted per measurement is plotted on fig 3. The S/N ratio is therefore around 100 for each  $2^\circ$  bin represented on fig.3. The absolute sensitivity is not known accurately, but corresponds roughly to one count for one Rayleigh of  $L\alpha$  intensity. Its exact value is irrelevant for the purpose of this paper since we are interested in the shape of the signal between scan angles  $120^\circ$  and  $240^\circ$ , corresponding to the upwind region from  $60^\circ$  below up to  $60^\circ$  above the ecliptic plane. A dip in the signal of about 10 % can be detected on each scan of fig.3, centered at scan angle  $180^\circ$  (in the ecliptic plane). This dip is quite obvious in sessions S-56 and S-74 where the region near the dip is free of stellar contamination. It is still also quite clear in session S-67 when star spikes are discarded near  $172^\circ$  and  $188^\circ$ .

For sessions S-56, S-67 and S-74 (respectively at dates 02/19/77, 03/05/77, 03/23/77), the ecliptic longitude of the scan plane were respectively  $237.6^\circ$ ,  $248^\circ$  and  $268.7^\circ$ . Focusing our interest only in the  $120^\circ$ - $240^\circ$  scan angle sections of the data curves (corresponding to  $60^\circ$  of latitude below and above the ecliptic plane), it is clear from fig. 1 that the three scan planes are cutting the MER region at various places around the upwind direction (at  $252^\circ$  of longitude). Therefore, we interpret the dips observed in the intensity as a general deficiency of H density near the

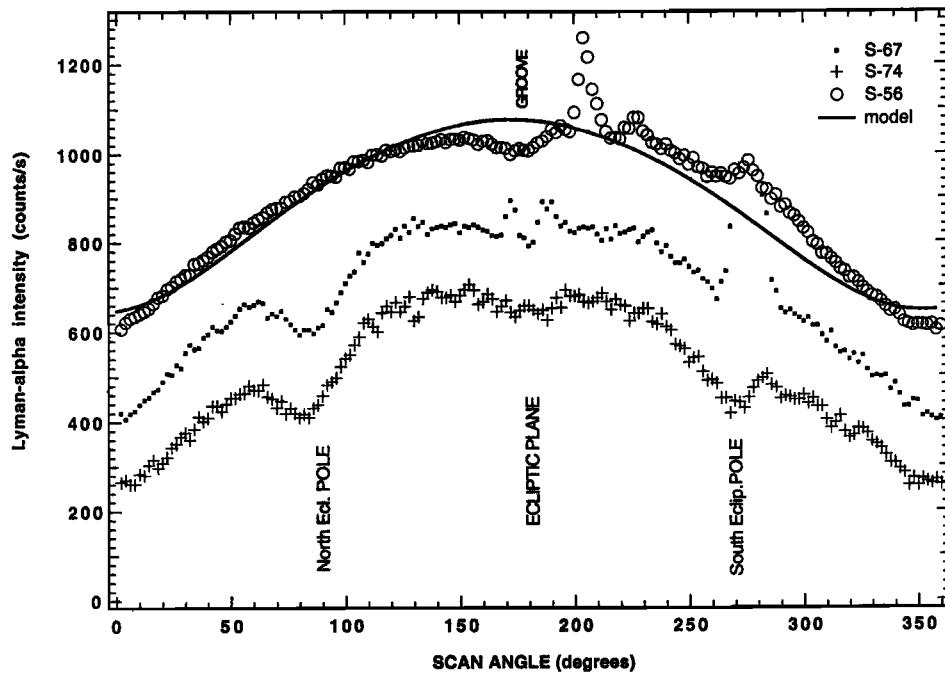


Figure 3. Interplanetary  $L\alpha$  intensity collected by Prognoz-5 at three positions of Figure 1, as a function of scan angle in planes perpendicular to the ecliptic ( $0$  and  $180^\circ$  in ecliptic ;  $+90^\circ$  is North Ecliptic pole,  $+270^\circ$  is South Ecliptic pole). Units are counts/sec. Curves for S-67 and S-56 are displaced respectively by 200 and 400 counts/s vertically for clarity. The effect of the H cell absorption on the interplanetary emission is clearly visible for S-67 and S-74 around  $+90^\circ$  and  $+270^\circ$ . In some cases, there are spikes due to hot stars ( $205^\circ$  for S-56,  $170^\circ$ - $190^\circ$  for S-67) and also some geocorona around  $270^\circ$ . All curves show a dip of intensity centered on the ecliptic plane, forming a groove in the Ly-alpha sky pattern. The solid line is a model curve for an isotropic solar wind.

ecliptic plane, affecting the whole MER region: a groove, which position is indicated on the model map (fig.2).

### Discussion

The groove detected in the  $L\alpha$  pattern with Prognoz-5 reflects a deficiency of emissivity, and therefore of neutral H, localized near the ecliptic plane in the MER region. This deficiency is the result of an enhanced ionization rate concentrated near the ecliptic plane. It cannot be an enhancement of the EUV ionization, first because EUV accounts for a small fraction of the ionization, and second because it would require an unrealistic distribution of the source of EUV radiation, with a very large concentration near the solar equator. This is because for a point in the ecliptic, one H atom receives EUV radiation from the whole solar disc (from all latitudes), while it is ionized by solar wind contained only in the ecliptic plane if it is located upwind from the sun, in the MER region. The same kind of argument can be used to exclude the possibility that the groove could be due to a variation of latitude of the illuminating solar  $L\alpha$ , as discussed by Pryor *et al.* (1992).

The first solar wind ionization rate latitude distribution which was used to interpret the polar enhancement of  $L\alpha$  emission were of the harmonic form:  $1 - A \sin^2 \lambda$  (Kumar and Broadfoot, 1979; Lallement *et al.*, 1985). However, the  $L\alpha$  intensity pattern which is computed with such a solar wind distribution does not show the  $L\alpha$  groove detected by Prognoz-5. In order to produce a groove, the distribution of the ionization rate must be much more peaked near the ecliptic plane than the harmonic form.

Indeed, it was found that, in order to fit the curves S-56 and 4 other curves of Prognoz-6 (not shown here), the

distribution of solar wind ionization rate and mass flux presented a strong peak in the ecliptic, bracketted by two constant plateaus from  $-90^\circ$  to  $-30^\circ$  and from  $+30^\circ$  to  $+90^\circ$  (Summanen *et al.*, 1993). Such a distribution, derived from the  $L\alpha$  sky pattern observed by Prognoz in 1977, is very similar to the distribution found in 1994 with *in-situ* measurements of the solar wind by Ulysses (Phillips *et al.*, 1995), once the following comment is taken into account: Ulysses solar wind data were collected from September 13, 1994 to July 31, 1995 during its ascension from  $-80^\circ$  to  $+65^\circ$  of latitude (Phillips *et al.*, 1995). Both the velocity and the density are relatively constant (at 750 km/s and  $2.5 \text{ cm}^{-3}$ ), except for the region from  $-20^\circ$  to  $+20^\circ$ , where the velocity drops to 400 km/s and the density increases up to  $8\text{-}12 \text{ cm}^{-3}$ , with strong fluctuations associated most likely with multiple crossings of the neutral sheet where the slow solar wind is concentrated. From these numbers, we derived a crude estimate of the average solar wind proton flux of  $3.2 \times 10^8$  protons  $\text{cm}^{-2}\text{s}^{-1}$  at 1 AU for the slow solar wind in the latitude band  $-20^\circ$  to  $+20^\circ$ , and  $2 \times 10^8$  protons  $\text{cm}^{-2}\text{s}^{-1}$  for the fast solar wind, outside this latitude band. This description seems to be in contradiction with one figure of Phillips *et al.* (1995), showing a pretty constant median value of the solar wind mass flux with latitude. We argue that, within the latitude band  $-20^\circ$  to  $+20^\circ$ , where strong fluctuations occur, the median value is necessarily smaller than the average value. In this respect, the representation of the median value of Phillips *et al.*, might have confused some people, since it could be interpreted as if Ulysses found a solar wind mass flux constant with latitude, while the detailed data show exactly the opposite: a strong increase confined around the neutral sheet.

Indeed, Phillips (private communication, 1995) was kind

enough to compute accurately the solar wind proton flux from Ulysses primary data during the South to North solar pass, by multiplying individual densities by individual velocities, and to communicate to us his results: the mean proton flux, averaged by solar rotation, is  $2.8 \times 10^8$  protons  $\text{cm}^{-2}\text{s}^{-1}$  (at 1 AU) between  $-20$  and  $+20^\circ$ , while it drops to a constant value of  $1.9 \times 10^8$  protons  $\text{cm}^{-2}\text{s}^{-1}$  above  $40^\circ$  of latitude in both hemispheres. Therefore, Ulysses demonstrates that there is a strong variation of the solar wind mass flux with latitude, the "classical" value ( $3 \times 10^8$  protons  $\text{cm}^{-2}\text{s}^{-1}$  found by scores of in-ecliptic instruments flown since several decades) being confined in a narrow band of latitude where the neutral sheet was found, with the rest of space having a smaller flux at  $2 \times 10^8$  protons  $\text{cm}^{-2}\text{s}^{-1}$ . Since the charge-exchange cross-section  $\text{H-H}^+$  decreases when the velocity increases, the Ulysses solar wind mass flux would result in an ionization rate enhanced by 75 percent in the ecliptic with respect to higher latitudes (including a 20 percent contribution of EUV photo-ionization).

In fact, the increased solar wind flux detected by Ulysses in the neutral sheet seems to be even more concentrated ( $\pm 20^\circ$ ) than the latitude extent (vertical width) of the  $\text{L}\alpha$  groove ( $\pm 40^\circ$ ), and the groove not as deep as the 75 % figure of the ionization rate. One reason is the velocity spread of interstellar H atoms due to their temperature of 8,000 K. The other is that the ionization effect of the solar wind is averaged over a few solar rotations (the lifetime of one H atom at the distance of the peak emissivity of the MER, typically 2.5 AU, is 107 days). Therefore, even if the neutral sheet is very narrow, the width and depth of the groove will depend on its particular configuration. In particular, its inclination to the heliographic equator is very important. It is related to the so-called tilt angle of the Heliospheric Current Sheet (HCS), identical to the neutral sheet mentioned above, which was calculated from large scale solar magnetic field photospheric measurements by Hoeksema (1991). At the beginning of 1977, it was about  $15^\circ$  only, increasing fast with the development of the solar cycle toward the maximum. Therefore, we may expect a solar cycle variation of the existence of the groove pattern. Near solar minimum, at the time when the tilt angle is zero, the HCS is completely flat, and perpendicular to the solar rotation axis, an ideal situation for the creation of the groove inside the MER, because points near the heliographic equator experience permanently a high and slow solar wind mass flux, giving a high ionization rate of incoming interstellar H atoms. When the tilt is increasing, the HCS becomes inclined and warped, and points in the MER region alternate between slow and fast solar wind, with a resulting smoothed ionization rate (the ionization time is larger than one solar rotation further out than 1 AU, from where comes the Lyman  $\alpha$  emission).

### Conclusion

A new feature of the sky  $\text{L}\alpha$  emission pattern was identified as a groove aligned with the ecliptic plane, ploughed across the upwind hemisphere, revealed by 1977 Prognos-5 data, thanks to the unique space resolution and high S/N ratio of the Prognos  $\text{L}\alpha$  photometer. This feature is interpreted as the result of increased ionization by charge-exchange with the slow solar wind of the neutral sheet, containing a higher mass flux as confirmed by Ulysses in 1995. Both periods were near a solar minimum, and the question of the permanent existence of this groove is raised, because it must depend on the configuration of the neutral sheet. The permanent monitoring of the MER region and the presence of the groove will be a prime target for forthcoming  $\text{L}\alpha$  observations with SWAN, on board the SOHO mission

(Bertaux et al, 1995). The *in-situ* results of Ulysses validated the  $\text{L}\alpha$  method as a powerful means for the remote-sensing determination of the large scale solar wind structure.

### Acknowledgements

The french  $\text{L}\alpha$  photometer was built at Service d'Aéronomie du CNRS with CNES funds and was placed on board Prognos-5 and 6 thanks to the efforts of the late Professor Shklovskii at IKI (Moscou) and Professor V.G. Kurt, to whom we wish to express our gratitude. We also would like to express our thanks to J.L. Phillips for the early communication of the average solar wind proton fluxes measured by Ulysses, and to Don Hassler for his revision of the style of this manuscript.

### REFERENCES

- Bertaux, J.L., R.Lallement, V.G., Kurt, and E.N. Mironova, Characteristics of the Local Interstellar Hydrogen determined from PROGNOZ 5 and 6 interplanetary Lyman  $\alpha$  line profile measurements with a hydrogen absorption cell, *Astron. Astrophys.*, 150, pp. 1-20, 1985.
- Bertaux J.L., R. Pellinen., E. Chassefière, E. Dimarellis, F. Goutail, T.E. Holzer, V. Kelha, S. Korpela, E. Kyrölä, R. Lallement, K. Leppala, G. Leppelmeier, I. Liede, K. Rautonen and J. Torsti, SWAN : A study of solar wind anisotropies, *Original proposal to ESA*, 1987 ; *The SOHO mission, ESA SP-1104*, 63-68, 1989.
- Bertaux, J.L., et al., (25 authors), SWAN : A study of solar wind anisotropies on SOHO with Lyman alpha sky mapping, *Solar Physics*, 162, 403-439 (1995)
- Hoeksema, J.T., Large scale solar and heliospheric magnetic fields, *Adv. Space Res.*, 17, n°1, 15-24, 1991
- Kumar, S. and A.L. Broadfoot, Evidence from Mariner 10 of solar wind flux depletion at high ecliptic latitudes, *Astrophys. J.*, 228, 302-311, 1979.
- Lallement R., J.L. Bertaux, V. G. Kurt, Solar Wind Decrease at High Heliographic Latitudes Detected from Prognos Interplanetary Lyman alpha Mapping, *J. Geophys. Res.*, 90, 1413-1423, 1985.
- Lallement R., J.L. Bertaux, E. Chassefière, B. Sandel, Interplanetary Lyman  $\alpha$  observations with UVS on Voyager : data, first analysis, implications for the ionization lifetime, *Astronomy and Astrophysics*, 252, 385-401, 1991
- Phillips J.L., S.J. Bame, A. Barnes, B.L. Barraclough, W.C. Feldman, B.E. Goldstein, J.T. Gosling, G.W. Hoogoven, D.J. McComas, M. Neugebauer, S.T. Suess, Ulysses solar wind plasma observations from pole to pole, *GRL*, 22, 3301-3304, 1995
- Pryor, W.R., J.M. Ajello, C.A. Barth, et al., The Galileo and Pioneer Venus ultraviolet spectrometer experiments : solar Lyman  $\alpha$  latitude variation at solar maximum from interplanetary Lyman- $\alpha$  observations, *Astrophys. J.*, 394, 363-377 (1992).
- Summanen T., R. Lallement, J.L. Bertaux and E. Kyrölä, Latitudinal Distribution of Solar Wind as Deduced from Lyman Alpha Measurement : An improved method, *J. Geophys. Res.*, 98-A8, pp. 13.215-13.224 (1993)

Jean-Loup Bertaux, Service d'Aéronomie du CNRS, Route Forestière de Verrières, BP3,91371 Verrières-le-Buisson, France; e-mail: bertaux@aerov.jussieu.fr

(received May 14, 1996; revised August 10, 1996; accepted August 21, 1996)